Applied Ocean Research 158 (2025) 104546

Contents lists available at ScienceDirect

Applied Ocean Research

journal homepage: www.elsevier.com/locate/apor

Observed changes in significant wave heights derived from long-term homogenized measurements offshore mainland Portugal

Rita Esteves [a], Diogo Mendes [b], Maria Graça Neves [c], Tiago Oliveira [d], José Paulo Pinto [a,*]

[a] Instituto Hidrográfico, Rua das Trinas 49, 1249-093 Lisboa, Portugal
[b] CERIS – Civil Engineering Research and Innovation for Sustainability, Instituto Superior Técnico, Lisbon, Portugal
[c] CERIS—Civil Engineering Research and Innovation for Sustainability, Department of Civil Engineering, NOVA School of Science and Technology, 2829-516 Caparica, Portugal
[d] Physics Department & Centre of Environmental and Marine Studies (CESAM), University of Aveiro, Portugal

ARTICLE INFO

Keywords:
Wave climate
North atlantic ocean
Long-term analysis
Wind-waves
Mann-kendall
RHTests

ABSTRACT

Trends in wind-wave climates across the globe have been primarily addressed using numerical models. Availability of long-term data collected by wave buoys is often scarce and they present inhomogeneities associated with wave buoy size and hardware over time. Here, a trend analysis was conducted on approximately 40 years of homogeneous wind-wave data collected by wave buoys offshore mainland Portugal. For that, a homogenization methodology based on RHTestsV4, with ERA5 wave hindcast as reference time series was used. Results indicate that along the north-western coastline facing the North Atlantic, an increasing trend of monthly mean significant wave height of +10 mm/yr was observed at FigLei record for the months between October and December. Along the south-western coastline, no statistically significant trends were observed. Along the southern coastline, which is also exposed to wind-waves generated in the Mediterranean Sea results at Faro record show a decreasing trend of monthly 90th percentile of -22.2 mm/yr between October and December. A further comparison between the wind-wave trends obtained with local wave buoys and those from the global ERA5 wave hindcast highlights that the trends of the later can be opposite, or they can vary by up to a factor of 10 which emphasizes the importance of long-term wave buoy observations networks for a more accurate understanding of local wave climates.

1. Introduction

The long-term analysis of wind-generated waves is essential for the assessment of trends and variability of the climate system (Young and Ribal, 2019). Moreover, this analysis is relevant for various ocean engineering endeavours impacting human activities. Examples include the design of offshore, coastal and harbour structures (CIRIA/CUR/CETMEF, 2007; DNV-RP-C205, 2019), the optimization of shipping routes to minimize travel time and fuel consumption (e.g., Taskar et al., 2023), the effective planning and deployment of wave energy for renewable energy generation (e.g., Ribeiro et al., 2020; Silva et al., 2022; Clemente et al., 2023), among others.

While wind-generated waves are a global phenomenon impacting oceans, seas and lakes, we focus on the offshore region of mainland Portugal located in the eastern North Atlantic Ocean (see Fig. 1). This focus emerges due to the availability of unique long-term wave buoy data in this specific area. Additionally, the number of long-term records from wave buoys is significantly smaller on the eastern than on the western North Atlantic Ocean (Casas-Prat et al., 2024). This later aspect precludes a throughout understanding of the wind-wave climate trends in this ocean basin.

Previous studies analysing long-term wave trends in the North Atlantic have employed various data sources like instrumental measurements, satellite altimetry and numerical wave hindcasts. Among the different bulk wave parameters of interest for ocean engineering applications, the spectral significant wave height (H_{m0}) based on the zeroth-moment of the wave spectrum has received the most attention. Instrumental measurements recorded at Seven Stones Light Vessel (i.e. 50.060° N; 6.072° W) revealed an increase in annual monthly mean H_{m0} of +22.0 mm/yr between 1962 and 1986 (Bacon and Carter, 1991). Within the scope of the WASA project, a 40 year reconstruction (1955 – 1994) of the wave climate in the northeast Atlantic reveals contrasting trends (Günther et al., 1997). Results suggest an upward trend around +5.0 to +10.0 mm/yr in 90-percentile H_{m0} and +2.0 to +5.0 mm/yr in

* Corresponding author.
E-mail address: paulo.pinto@hidrografico.pt (J.P. Pinto).

https://doi.org/10.1016/j.apor.2025.104546
Received 25 July 2024; Received in revised form 28 February 2025; Accepted 24 March 2025
Available online 31 March 2025

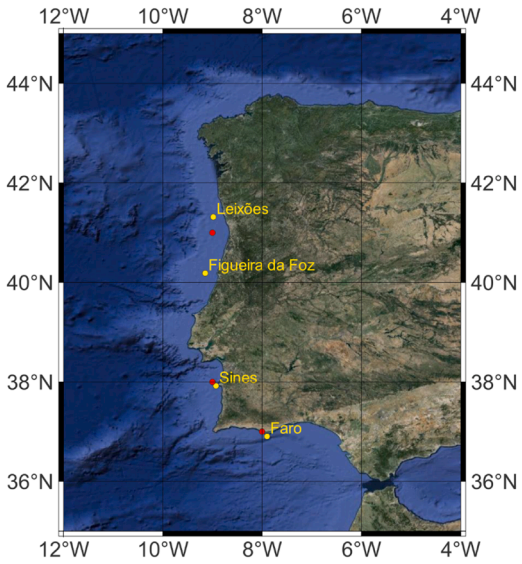

Fig. 1. - Geographic location of mainland Portugal, wave buoys located on the continental shelf (yellow dots) and ERA5 wave hindcast points (red dots).

mean H_{m0} at the North Sea and Norwegian Sea.

In the westernmost areas below latitude 55°, between Ireland and North Iberia, it is found a decrease from −5.0 to −15.0 mm/yr in 90-percentile H_{m0} and −5.0 mm/yr in mean H_{m0}, with the exception of the Bay of Biscay where there is an increase of +2.5 mm/yr. Sterl et al. (1998) employed a 15-yr global wave hindcast. Their results revealed an increase in January monthly mean H_{m0} of +120.0 mm/yr for the northeastern North Atlantic (1979–1994) but with large monthly variability. Importantly, both Günther et al. (1997) and Sterl et al. (1998) results highlighted the significant spatial variability of trends within the North Atlantic.

A subsequent 40-yr global wave hindcast by Wang & Swail (2001) revealed an increase in winter (i.e. January, February and March - JFM) seasonal 90-percentile H_{m0} at high latitudes. This increase reached up to +50.0 mm/yr (200 cm in 40-yr) and contrasted with a decrease of −20.0 mm/yr at low latitudes between 1958 and 1997. Further supporting the contrasting trends between high and low latitudes, Dodet et al. (2010) conducted a 57-yr wave hindcast for the North Atlantic (1953–2009). Their analysis revealed that the 90-percentile H_{m0} increased at 45° N, 12.5° W (+2.0 mm/yr), while it decreased at 35° N, 12.5° W (−2.0 mm/yr).

A subsequent 109-yr wave hindcast by Bertin et al. (2013) highlighted a consistent increase in mean H_{m0}. This increase ranged from 2.0 mm/yr at 30° N to 8.0 mm/yr at latitudes above 55°N. Martínez-Asensio et al. (2016) employed a wave hindcast with ERA-Interim wind fields, pointing out a spatially variable pattern in winter (i.e., December, January, February and March - DJFM) H_{m0} trends. These trends ranged from a decrease of −10.0 mm/yr to an increase of +10.0 mm/yr across most regions. Notably, a striking decrease of −50.0 mm/yr was observed by previous authors close to the North Pole (Martínez-Asensio et al., 2016).

Satellite altimetry studies also indicated the spatial variability in North Atlantic wave height trends. Young & Ribal (2019) reported a global increase in mean and 90-percentile H_{m0} based on data between 1985 and 2018. In the North Atlantic, their results suggest an increase of about +3.0 mm/yr in mean H_{m0} and an increase of +10.0 mm/yr in 90-percentile H_{m0}. Analysing winter (JFM) trends specifically in the North Atlantic (1993–2018) with the ESA Sea State CCI v1 satellite derived product, Hochet et al. (2021) found increases of up to +20.0 mm/yr in some regions (i.e. western North Atlantic and Mediterranean Sea), contrasting with a decrease near the North Pole (−40.0 mm/yr). Table 1 provides a summary of the above-mentioned studies.

The studies included in Table 1 were carried out for the present-day climate. Future wind-wave trends are studied using Global Climate Models (GCMs). In this case, surface wind fields are used to force phase-averaged wave models, thereby projecting the future wind-wave conditions until the end of the 21st century (e.g., Aarnes et al., 2017; Morim et al., 2020; Meucci et al., 2023). Specifically for the north-eastern Atlantic, these climatic studies project a decrease of mean H_{m0} (Aarnes et al., 2017; Bricheno and Wolf, 2018; Bernardino et al., 2023). In what concerns higher percentiles of H_{m0}, previous studies using climate projections show both increasing trends (Bricheno and Wolf, 2018; Bernardino et al., 2023; Meucci et al., 2023) and decreasing trends (Aarnes et al., 2017) for this region. Wind-wave trends obtained using climatic models are also subjected to uncertainties, such as the IPCC emission scenarios, the phase-averaged wave model and the projections of the wind fields (Bitner-Gregersen et al., 2018).

Currently available global wave hindcasts provide extensive coverage, with ERA5 extending back to 1940 (Hersbach et al., 2020). These hindcasts combine numerical models with satellite observations through data assimilation techniques to improve predictions (Law-Chune et al., 2021). Nevertheless, for the region offshore mainland Portugal, wave hindcasts tend to underestimate both the largest values of H_{m0} measured by wave buoys (Dodet et al., 2010; Silva et al., 2022) and the values of H_{m0} during post-tropical storm waves (Oliveira et al., 2020; Campos et al., 2022), but they can also overestimate the maximum values of H_{m0} during extratropical storms (S. Ponce De León and Guedes Soares, 2014). Global numerical models are also less reliable in shallow waters (i.e. continental shelf) and inner seas and are inherently associated with errors that arise from their numerical discretization (Cavaleri et al., 2018). Additionally, global models are used with a spatial resolution that is often too coarse to provide sufficient details near the shore. In this regard, it is poorly understood how wind-wave trends obtained from global models, such as the ERA5 wave hindcast,

Table 1
– Summary of wind-wave trends of monthly mean and 90-percentile of significant wave height (H_{m0}) from previous studies in the North Atlantic Ocean based on instrumental measurements, wave hindcasts and satellites.

Source	Method	Period	Location	mean H_{m0} (mm/yr)	90-percentile H_{m0} (mm/yr)
Bacon and Carter (1991)	Instrumental measurements	1962–1986	6.1° W, 50.1°N	+22.0	–
Günther et al. (1997)	Wave hindcast	1955–1994	North Sea	+2.0 to +5.0	+5.0 to +10.0
			Ireland to North Iberia	−5.0	−15.0 to −5.0
Sterl et al. (1998)	Wave hindcast	1979–1994	northeastern North Atlantic	+120.0 (January)	–
Wang and Swail (2001)	Wave hindcast	1958–1997	High latitudes	–	+50.0 (JFM)
			Low latitudes	–	−20.0 (JFM)
Dodet et al. (2009)	Wave hindcast	1953–2009	12.5° W, 45°N	–	+2.0
			12.5° W, 35°N	–	−2.0
Bertin et al. (2013)	Wave hindcast	109-yr	> 30°N	+2.0	–
			> 55°N	+8.0	–
Martínez-Asensio et al. (2016)	Wave hindcast			−10.0 to +10.0 (DJFM)	–
Young and Ribal (2019)	Satellite altimetry	1985–2018	North Atlantic	+3.0	+10.0
Hochet et al. (2021)	Satellite altimetry	1993–2018	North Atlantic	+20.0 (JFM)	–

compare with local datasets.

Wave buoys are generally considered the most reliable source of wave data, despite limitations in spatial coverage and temporal gaps. These gaps are typically associated with very rough wave conditions, ship collisions or buoy maintenance periods. Additionally, long-term wave buoy records are rare as only less than 5 % of available global wave buoys have more than 40 years of data (Casas-Prat et al., 2024). Furthermore, data homogeneity is crucial when analysing long-term trends from wave buoy records. Studies by Liu et al. (2023) and Stopa et al. (2019) highlight the issue of temporal inhomogeneity in long-term wind-wave measurements caused by changes in software or hardware over time. This emphasizes the need for careful data quality control when using buoy data for long-term trend analysis. For instance, Gemmrich et al. (2011) demonstrated that inhomogeneity in buoy records from the northeast Pacific Ocean could explain half of the increasing wave height trend previously observed by Ruggiero et al. (2010).

In this paper, our objective is to analyse long-term trends in monthly mean, 90-percentile and 10-percentile H_{m0} offshore mainland Portugal. Specific objectives are as follows. First, we intend to perform an assessment of non-climatic changes in a long-term wind-wave dataset that was collected using wave buoys from the same manufacturer. Second, we aim to compare wind-wave trends obtained using local wave buoys with those obtained with the global ERA5 wave hindcast and with those obtained using climatic models. The focus is the eastern North Atlantic Ocean because our dataset has been collected in this region. To address the temporal inhomogeneities associated with wave buoy records, we applied the RHTestsV4 homogenization methodology (X. Wang and Feng, 2013) as previously used by Gemmrich et al. (2011) to a nearly 40-year dataset, consisting of four wave buoys deployed at approximately 100 m water depth.

The paper outline is as follows. Section 2 briefly introduces the wave climate offshore mainland Portugal, describes the wave buoy data and the employed methods to carry out the analysis. Section 3 presents the results for monthly mean, 90-percentile and 10-percentile H_{m0}, both for annual and seasonal time scales. Section 4 discusses the homogenization methodology and its relationship with known buoy changes over time and the differences between our regional results and other global studies obtained for the eastern North Atlantic. Section 4 also discusses the differences and similarities of wave trends between wave buoys and the ERA5 wave hindcast. Section 5 closes with the main conclusions.

2. STUDY AREA, DATA AND methods

2.1. Brief overview of the study area

Mainland Portugal is bordered by the North Atlantic Ocean (Fig. 1). The wave climate can be divided in two different wave regimes. The energetic wave regime along the western coastline, fully exposed to waves generated in the North Atlantic Ocean and the milder wave regime along the southern coastline. The latter is sheltered from northwest incident waves that were generated in the North Atlantic Ocean but it is exposed to southeastern wave systems generated in the Mediterranean Sea (Oliveira et al., 2018). An analysis of offshore wave buoys located in water depths between 1200 m and 1900 m, covering a time period between 2009 and 2020, highlights not only the differences between these two wave regimes but also the strong seasonality between winter and summer months (Mendes and Oliveira, 2021). While along the western coastline, the February value of $H_{m0} = 3.45 \pm 1.49$ m, it decreases to 1.62 ± 0.65 m in July.

For the southern coastline, the largest value occurred in March with 2.17 ± 1.02 m and the smallest in July with 1.16 ± 0.41 m. Two extreme events clearly highlight the energetic wave climate in the study area. The maximum value of H_{m0} recorded between 2009 and 2020 was 12.72 m during Storm Gong on 19th January 2013 at 11:00 (UTC +00h00) (Mendes and Oliveira, 2021). This record was obtained at Nazaré offshore wave buoy, located 90 km south of Figueira da Foz at 2000 m water depth (Fig. 1). Moreover, H_{m0} reached a value of 12.80 m during Storm Christina (often referred as Storm Hercules) on 1st February 2014 at 21:00 (UTC +00h00) (Sonia Ponce De León and Guedes Soares, 2015). The later record was obtained at Estaca de Bares buoy, that is moored at a water depth of 1800 m and located in northwest location of Spain.

2.2. Wave buoy measurements

In the Portuguese marine waters, there is an integrated permanent monitoring system (MONIZEE infrastructure), which includes 16 moored buoys equipped with wave, temperature, currents and meteorological sensors. It has contributions from the Hydrographic Institute (Instituto Hidrográfico - IH), that manages the moored buoy network in mainland Portugal, the University of Azores (Universidade dos Açores - UAC), and the Ports Administration of the Madeira Autonomous Region (Administração dos Portos da Região Autónoma da Madeira – APRAM). Oceanographic buoys are located in coastal (i.e., Datawell Waverider) and offshore (i.e., Oceanor Wavescan) regions of interest and close to harbour entrances. Our study focused on the coastal buoys located offshore mainland Portugal in water depths of about 100 m because those have approximately 40 years of data (Fig. 1 and Table 2).

The data used in this analysis were all acquired by Datawell buoys. Before 1986, the data were obtained by Datawell Waverider non-directional buoys, measuring only the vertical displacement. In 1986, the first directional buoy (Datawell Wavec), which measured both vertical and horizontal displacement, was installed in Faro. From 1986 to 1990, all the other buoys were gradually replaced with directional buoys. The mooring location was changed slightly over the years due to operational problems. The reference location for each buoy is shown in Table 2.

To ensure data homogeneity, the processing scheme remained unchanged. The buoys record the three-axis acceleration, subsequently converted on-board into a vertical displacement and two horizontal displacements, with a sampling rate of 1.28 Hz for 30 min. Under non-storm conditions this acquisition is made every hour. During storm conditions the acquisition rate changes to 30 min.

The displacement time series are transmitted in real-time through the VHF signal to a shore station and then sent to the IH office. Once received, the displacement time series undergo rigorous quality control procedures in line with international standards (UNESCO, 1993; US Integrated Ocean Observing System, 2019). After the displacement time series have been validated, wave parameters are estimated in time and frequency domains, considering 127 frequency bands for directional buoys (81 or 76 frequency bands for non-directional buoys). The displacement time series, the wave spectrum, and bulk wave parameters have all been stored in the IH office since 1980.

Considering that the Figueira da Foz and Leixões buoys were installed relatively close to each other, with similar depths of deployment and wave conditions, the two records were merged, resulting in a time series of 42 years (hereafter referred to as FigLei). Sines has 43

Table 2
- Moored buoy location, depth and history of non-directional and directional buoy.

Buoys	Location	Depth (m)	Non-Directional	Directional
Leixões	41° 19.00′N/08° 59.00′W	83	–	07/1996 - present
Figueira da Foz	40° 11.133′N/09° 08.733′W	92	06/1981 - 03/1990	07/1990- 02/1996
Sines	37° 55.267′N/08° 55.733′W	97	02/1980 - 05/1988	05/1988 - present
Faro	36° 54.283′N/07° 53.900′W	93	–	09/1986 - present

years of data, and Faro has 37 years.

Long records of wave data in these locations, spanning more than 30 continuous years, are available with some gaps. These gaps are due to occasional failures of the buoy resulting from human activities, such as ship collisions or mooring cut-offs or natural events, such as extreme storms. The severe operating environment in the eastern North Atlantic makes it challenging to maintain a long and continuous time series of wave data. Therefore, it is essential to evaluate the number of valid observations in the time series. The percentage of valid registered data during the analysed period is 76 % in FigLei, 80 % in Sines, and 77 % in Faro.

2.3. Wave data

2.3.1. Buoys

For each wave buoy record (i.e. FigLei, Sines and Faro), consisting of H_{m0} values every three hours, we computed the mean, the 90-percentile and 10-percentile of H_{m0} for each month. These variables were calculated only if the monthly data coverage is larger than 60 %. Hereafter, we will use the monthly mean of H_{m0}, the monthly 90-percentile of H_{m0} and the monthly 10-percentile of H_{m0} in the subsequent analysis.

2.3.2. ERA5 wave hindcast

Similar to the wave buoys, the monthly mean of H_{m0}, the monthly 90-percentile of H_{m0} and the monthly 10-percentile of H_{m0} were calculated for the ERA5 wave hindcast (Hersbach et al., 2020). ERA5 is a global wave hindcast dataset developed by the European Centre for Medium-Range Weather Forecasts. It provides a comprehensive picture of historical wave conditions worldwide, covering the period from 1979 to present. ERA5 wave model incorporates data assimilation through a wide range of observations, including satellite altimeter data and wave buoy measurements. This integration of various data sources allows ERA5 to accurately capture both small-scale and large-scale features of the global wave climate accurately. The ERA5 global wave hindcast dataset has a regular latitude-longitude grid of 0.5°. In this study, we selected the locations as close as possible to the wave buoys to ensure that the wave data used in our analysis closely represents the conditions experienced at each buoy location (see red markers in Fig. 1). Also, we used the period between 1980 and 2023 of the ERA5 wave hindcast.

2.4. Homogenization using RHTestsV4

The RHTestsV4 was chosen to test data homogeneity (X. Wang and Feng, 2013). This technique was used to detect and adjust local non-climate shifts in time records acquired by instrumental measurements. Although originally applied in the field of meteorology, RHTestsV4 can be used for dealing with different types of climate series. In particular, it has been employed to check wave records for homogeneity (e.g., Gemmrich et al., 2011). This method identifies statistically significant deviations even in the absence of supporting metadata; these are called Type 1 change points. Deviations not identified in the first level of analysis but statistically significant if supported by reliable metadata are called Type 0 change points. As a rule, Type 1 change-points are all accepted but Type 0 change-points are only accepted if supported by metadata.

For each record, the homogeneity test has been performed on the monthly mean H_{m0} ($<H_{m0}>$). To increase sensitivity and reliability in the detection of non-climate shifts in time, a reference series was used based on the ERA5 wave hindcast (H_{ref}). In this scheme, the penalized maximal *t*-test is employed to find unknown change points in the base-minus-reference series, defined by $\langle \Delta H_{m0} \rangle = \langle H_{m0} \rangle - H_{ref}$, and to assess the significance of those changes (X. L. Wang, 2008; X. L. Wang et al., 2007). The method assumes zero-trend for the $\langle \Delta H_{m0} \rangle$ series and that both series should have a linear trend of the same order of magnitude. Instead of the mean-shift adjustment provided in the previous versions of RHTests, the quantile-matching (QM) adjustment algorithm implemented in RHTestsV4 was used to correct the non-homogeneities found in the datasets (Vincent et al., 2012; X. L. Wang et al., 2010). The QM scheme could account for seasonal modulation, adjusting winter and summer differently. For all records, the choice of the data segment for which the series is to be adjusted always corresponds to the most recent. This procedure is only validated if the corrected series is tested homogeneously.

2.5. Trend analysis of wave data

Similar to previous studies (e.g., Young and Ribal, 2019), wind-wave trend analysis was carried out using the Mann-Kendall test (Mann, 1945) to assess statistical significance and Sen's slope (Sen, 1968) to obtain the trend. The analysis was performed to identify yearly, semi-annual and quarterly trends based on monthly mean, 90-percentile and 10-percentile of H_{m0}.

For the annual trends, wave buoy records may not have a monthly data coverage larger than 60 % for a complete year (i.e., between January and December). Therefore, we followed the procedure detailed in Bacon & Carter (1991). Annual average values of mean, 90-percentile and 10-percentile of H_{m0} were formed using twelve consecutive months with a minimum monthly percentage of valid data equal to 60 %. Overall, from the approximately 40 years of data, about 20 full years were considered on each record.

For the semi-annual trends, summer was defined as the months between April to September, and winter between October and March. For the quarterly trends, Spring was April, May and June (AMJ), Summer was July, August and September (JAS), Autumn was October, November and December (OND) and Winter as January, February and March (JFM). We also noted that previous studies (Table 1) have calculated trends for an intermediate winter, covering the months of December, January, February and March (DJFM). We also considered this period in the analysis. Semi-annual and quarterly trends used the averaged values of mean, 90-percentile and 10-percentile of H_{m0} if the monthly data coverage for the several months included in each period was larger than 60 %.

The monthly mean H_{m0} for the three wave records clearly shows two distinct patterns (Fig. 2). Firstly, the strong seasonality between winter and summer. Secondly, the milder wave climate at Faro when compared to FigLei and Sines. Moreover, the largest values took place during February 2014, which was a very stormy winter along the eastern North Atlantic (Masselink et al., 2016; Oliveira et al., 2018). Additionaly, the largest amounts of insufficient data coverage mainly occurred between 1990 and 2000 for the three wave records.

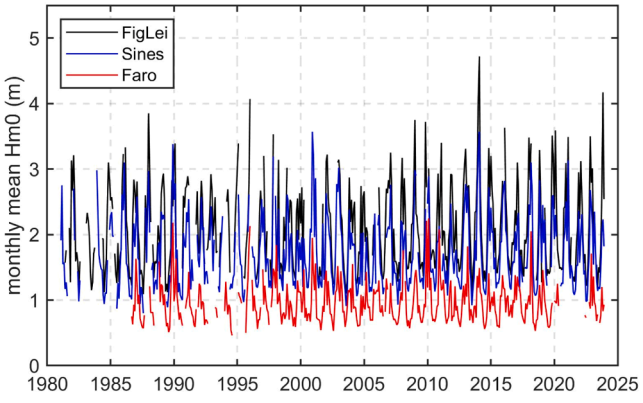

Fig. 2. – Homogenized monthly mean H_{m0} for FigLei, Sines and Faro wave records. Blank spaces are associated with a monthly data coverage smaller than 60 %.

3. results

3.1. Comparison between wave buoys and ERA5 wave hindcast

As shown in Fig. 3, the monthly mean H_{m0} for non-homogenized wave buoy records with monthly data coverage larger than 60 % match well with the ERA5 wave hindcast. In Fig. 3 and Table 3, the standard error metrics bias, root-mean square error (rmse) and normalized rmse (nrmse), see Appendix A, where the normalization was performed with the mean value of the observations, related to the buoy and ERA5 comparison are presented. Along the western coastline (i.e. FigLei and Sines), the ERA5 wave hindcast compare well with observed monthly mean H_{m0} with an underestimation at FigLei (bias = −0.16 m) and an overestimation at Sines (bias = 0.09 m). Nevertheless, the nrmse values were smaller than 10 % on both records. At Faro, the ERA5 hindcast shows a bias = −0.18 m, which is very close to the rmse = 0.21 m (Fig. 3). For FigLei and Faro, differences between ERA5 and wave records start to increase when the comparison is performed with the monthly 90-percentile and further decrease for the monthly 10-percentile (Table 3).

For Sines, the differences start to increase for the monthly 10-percentile when compared to the monthly mean and 90-percentile. Overall, differences between wave buoys and ERA5 wave hindcast presented for the study area (Fig. 3 and Table 3) closely follow previous studies. In more details, Kodaira et al. (2023) compared four wave model hindcasts, including the ERA5, against wave buoys. These authors highlighted the good agreement of mean H_{m0} between wave buoys and the ERA5 wave hindcast for the Northeast Atlantic. This agreement worsens for larger values of H_{m0}, where the ERA5 wave hindcast typically showing an underprediction (see their Fig. 6).

3.2. Homogenized wave data from buoys

The homogeneity of the wave records was calculated for FigLei, Sines and Faro (Section 2.4). No change points were identified. The homogeneity of H_{ref} was verified for all wave stations and a type 0 change-point was found for FigLei and Faro records in May and November 2003, respectively. However, both change points are inconclusive and not statistically relevant. They can only be significant if supported by reliable metadata.

The deviations found in H_{ref} can be partially explained by the number of data assimilated in the ERA5 wave hindcast. These increased from 0.75 million per day in 1979 to 24 million per day in 2019 with some discontinuities that may influence the performance of the wave climate reanalysis (Hersbach et al., 2020). However, as most updates were carried out over time and not at a particular moment, it was decided to use the ERA5 wave hindcast as the reference time series.

Time series of H_{m0} show a large seasonal dependence with significant multi-annual fluctuations, especially in winter (Fig. 4, top panel). This seasonal modulation is also visible in the monthly mean H_{m0} record. To identify the positions and significance of step-like change-points in $\langle H_{m0} \rangle$ datasets, the RHTestsV4 was applied using the base-minus-reference series ($<\Delta H_{m0}>$). Statistically significant deviations even in the absence of supporting metadata (Type 1 change-points) occurred for FigLei, Sines and Faro records. Type 0 change-points identified in Sines and Faro were related to changes in the type of buoy (see Table 4). The positions of change-points and corresponding mean shifts is illustrated in Fig. 4-mid panel for the Sines record.

According to available metadata, Leixões and Sines stations switched from non-directional WAVERIDER to directional WAVEC in July 1990 and April 1988, respectively. Later, all stations switched from directional WAVEC to directional WAVERIDER; FigLei in February 1998, Sines in March 1996 and Faro in February 2000. Additionally, FigLei record changed location from Figueira da Foz to Leixões in June 1996.

The homogeneity of the $\langle H_{m0} \rangle$ time records is obtained through the QM algorithm available in the RHTestsV4 package. Fig. 5 depicts the estimated adjustment for each record. Regarding the last twenty years, the results suggest that during the first two decades buoys generally overestimate $\langle H_{m0} \rangle$. However, these deviations are dominated by Type 1 change-points without metadata to justify it (see Table 4).

A linear interpolation of the QM adjustments was considered to correct the original H_{m0} three-hour series. This procedure made it possible to estimate the monthly 90th percentile and 10th percentile of H_{m0} based on the homogenized monthly series.

3.3. Wave trends based on wave buoy records and ERA5 wave hindcast

Unless explicitly stated, the results included in this section are only those associated with the wave buoy records that displayed statistically

Table 3
– Error metrics between ERA5 wave hindcast and non-homogenized buoy records.

Monthly 90-percentile H_{m0}			
	FigLei	*Sines*	*Faro*
bias (m)	−0.40	0.03	−0.39
rmse (m)	0.49	0.20	0.48
nrmse (-)	0.15	0.07	0.30
Monthly mean H_{m0}			
	FigLei	*Sines*	*Faro*
bias (m)	−0.17	0.09	−0.18
rmse (m)	0.23	0.14	0.22
nrmse (-)	0.11	0.08	0.23
Monthly 10-percentile H_{m0}			
	FigLei	*Sines*	*Faro*
bias (m)	0.02	0.15	−0.04
rmse (m)	0.10	0.18	0.06
nrmse (-)	0.09	0.19	0.13

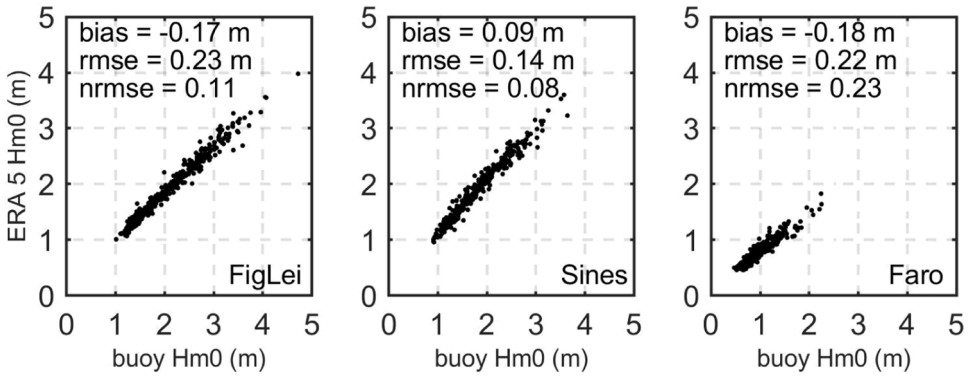

Fig. 3. – Scatter plot between ERA5 wave hindcast and non-homogenized buoy record monthly mean H_{m0} for FigLei, Sines and Faro wave records, with error metrics.

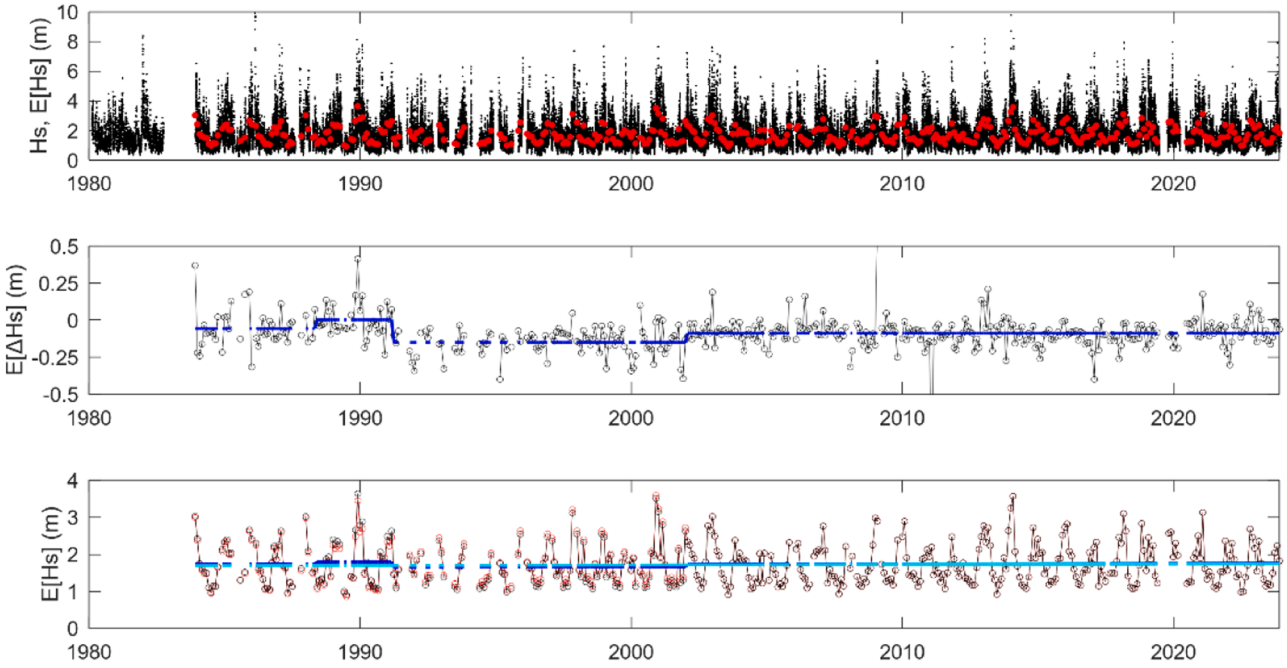

Fig. 4. - RHTestsV4 results for Sines record. Top panel: Time series of H_{m0} (black dots) and the monthly mean H_{m0} (red dots). Mid panel: Mean shifts (blue line) and change-points of the base minus reference series. Bottom panel: Original (black dots) and QM adjusted (red dots) monthly mean H_{m0}; Multi-regression trend of the original monthly series (blue line) and linear trend fit to the de-seasonalized adjusted monthly series (cyan line).

Table 4
- Date, type and step size of changes of points according to RHTestsV4 scheme for different buoys.

Buoy	*Date*	*Type*	*Step size (m)*	*Metadata*
FigLei	August 1988	1	−0.09	–
Sines	May 1988	0	0.06	switch to directional WAVEC
	March 1991	1	−0.15	–
	January 2002	1	0.06	–
Faro	February 1998	1	−0.13	–
	January 2000	0	0.08	replace WAVEC by WAVERIDER

significant trends at 95 % level. The remaining trends for annual, semi-annual and quarterly time periods, both for wave buoy records and ERA5 wave hindcast, of monthly mean, 90-percentile and 10-percentile H_{m0}, and the associated p-value can be found in Appendix B. The homogenized wave buoy records were used hereafter.

The annual FigLei record is composed of 18 complete years (see Section 2.5). No statistically significant annual trends were found for monthly mean, 90-percentile or the 10-percentile H_{m0} (see Appendix B). Semi-annual trends were also not statistically significant for this record. For the quarterly trends, a statistically significant value of monthly mean H_{m0} for OND quarter was found (Fig. 6a). This upward trend was of +10.0 mm/yr (p-value = 0.047) and it was based on 27 years. The ERA5 wave hindcast between 1980 and 2023 displayed an upward trend of +5.0 mm/yr that is not statistically significant (Fig. 6a).

The Sines record did not show any yearly, semi-annual or quarterly statistically significant trend (see Appendix B).

Unlike FigLei and Sines wave records, Faro record was obtained along the southern coastline (see Fig. 1). An annual trend was observed for the monthly 10-percentile H_{m0}. This upward trend, composed of 19

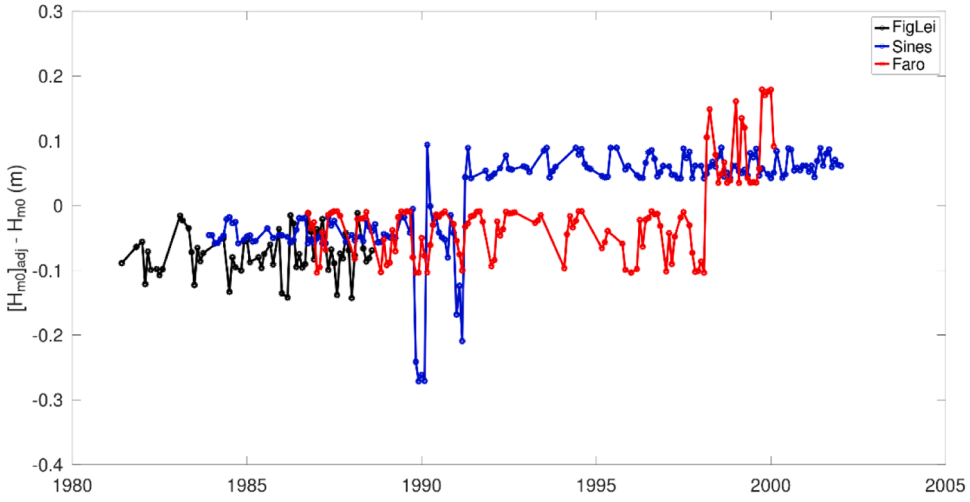

Fig. 5. - RHTestsV4 QM adjustments for all stations.

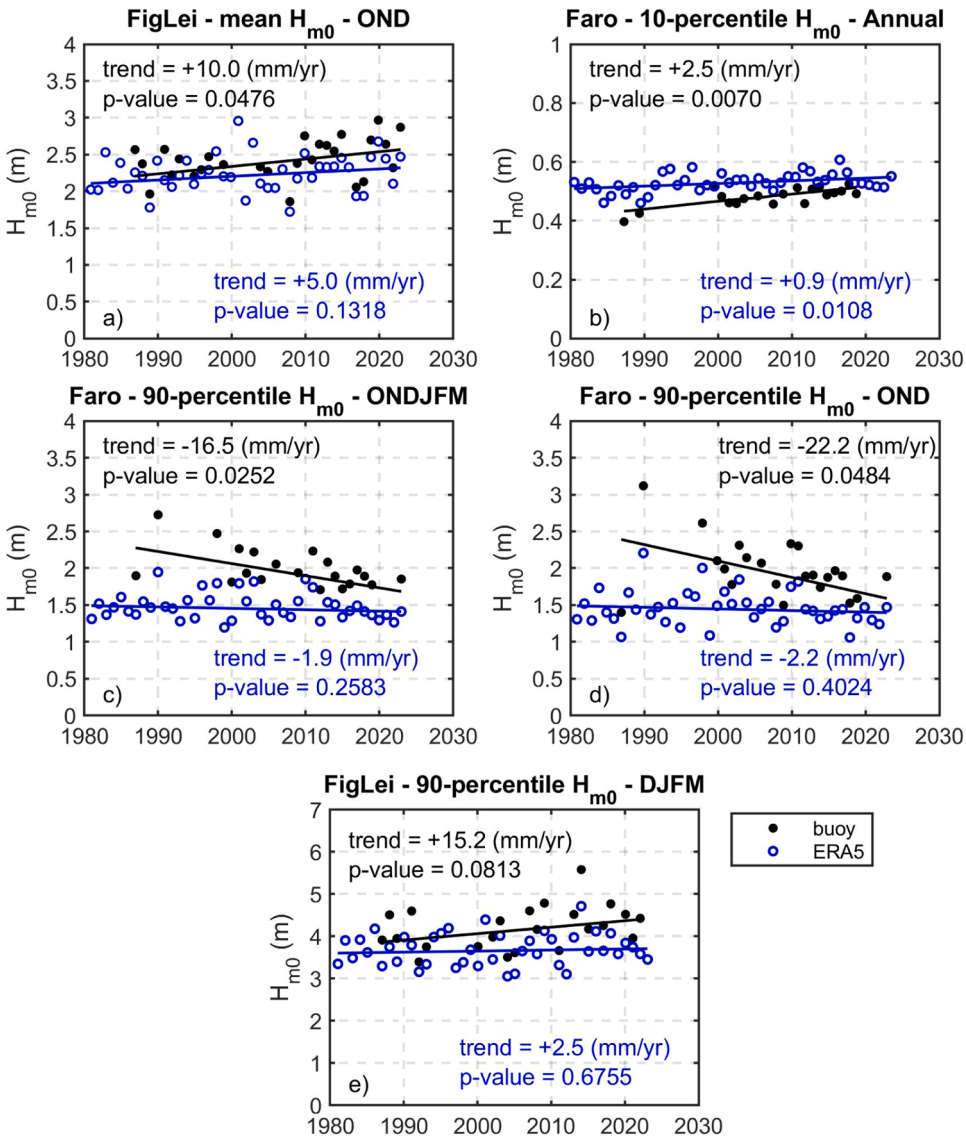

Fig. 6. – Monthly trends of wave buoy records (black) and ERA wave hindcast (blue): mean H_{m0} for OND quarter on FigLei record (a); 10-percentile H_{m0} on annual Faro record (b); 90-percentile H_{m0} for ONDJFM semester on Faro record (c); 90-percentile H_{m0} for OND quarter on Faro record (d); 90-percentile H_{m0} for DJFM on FigLei record (e). The linear trend and p-value are also shown.

complete years, is of +2.5 mm/yr (p-value = 0.007). The ERA5 wave hindcast was associated with an upward trend of +0.9 mm/yr (p-value = 0.0108) (Fig. 6b).

Moreover, two semi-annual statistically significant trends were observed. The first is a + 1.8 mm/yr (p-value = 0.015) of monthly 10-percentile H_{m0} during summer months (between April and September) (see Appendix B). The ERA5 wave hindcast also displayed this statistically significant upward trend (+0.6 mm/yr; p-value = 0.0409). The second is of −16.5 mm/yr (p-value = 0.0252) of monthly 90-percentile H_{m0} during winter months (Fig. 6c). The ERA5 wave hindcast also displayed a downward trend of −1.9 mm/yr but not statistically significant at 95 % level (p-value = 0.2583).

For the quarterly time periods, three statistically significant trends were obtained. The first two were the upward monthly 10-percentile H_{m0} for JFM and AMJ of +2.8 mm/yr and +2.2 mm/yr, respectively (see Appendix B). These two quarterly trends agree with the semi-annual and annual trends obtained earlier (see Fig. 6b). The ERA5 wave hindcast only detected an upward trend of monthly 10-percentile H_{m0} for the AMJ quarter of +0.8 mm/yr (p-value = 0.0216).

The third statistically significant trend was obtained for the OND quarter. This trend of −22.2 mm/yr (p-value = 0.0484) was obtained for the monthly 90-percentile H_{m0} (Fig. 6d). Similar to the results obtained for the semi-annual trend (Fig. 6c), the ERA5 wave hindcast detected a downward trend of monthly 90-percentile H_{m0} for the OND quarter of −2.2 mm/yr that is not statistically significant (p-value = 0.4024).

Instead of using the JFM quarter to characterize winter months, some authors have used the months of December, January, February and March to characterize winter conditions (Martínez-Asensio et al., 2016). When analysing the DJFM period, FigLei record showed two statistically significant trends at 90 % level. The first is an increase of +10.3 mm/yr in the monthly mean H_{m0} (p-value = 0.0538). The second is the increase of +15.3 mm/yr in the monthly 90-percentile H_{m0} (p-value = 0.0831) (Fig. 6e). The ERA5 wave hindcast also displayed an increasing trend but not statistically significant.

For the DJFM period and as above, Sines did not show any statistically significant trends. Regarding Faro, an upward trend of +3.1 mm/yr (p-value = 0.0217) for the monthly 10-percentile H_{m0} for the DJFM period (see Appendix B). The ERA5 wave hindcast also showed this increasing trend of +0.8 mm/yr but not statistically significant (p-value = 0.2669).

4. Discussion

4.1. Homogeneity of wave buoy records

A key aspect of this study was the homogenized methodology applied to three long-term wave buoy records, obtained offshore mainland Portugal, to account for non-climatic changes. Similar to previous studies, like Gemmrich et al. (2011) that used the OceanWeather GROW2000 wave hindcast, we used a reference time series based on the ERA5 wave hindcast. The largest step changes in Gemmrich et al. (2011) were about plus or minus 0.6 m, after an analysis of seven offshore wave buoys located in the eastern North Pacific Ocean. In their study, this large step changes occurred after a change in the hull, payload and processor of the wave buoy. The maximum step change in our study was −0.16 m for the Sines location. We attribute this smaller step change to the wave buoy manufacturer. In our case, only Datawell wave buoys were used. Even using only buoys from the same manufacturer, two step changes took place. At Sines, a step change of 0.06 m occurred in May 1988 when the non-directional wave buoy was replaced by directional WAVEC wave buoy. At Faro, a step change of 0.08 m took place in January 2000 when the WAVEC wave buoy was replaced by the WAVERIDER wave buoy. Our analysis also indicated non-climatic step changes at FigLei, Sines and Faro wave records not associated with metadata. The reason for this remains unknown.

The changepoint found in the FigLei record is two years before the non-directional WAVERIDER to directional WAVEC switch, even after considering the date of this change in RHTestsV4. Although the switch from WAVEC to directional WAVERIDER was made in all records, only Faro record shows a non-homogeneity linked with this replacement.

Fig. 4-bottom panel shows for Sines the multi-phase linear regression trends and the de-seasonalized linear trend fit to the adjusted monthly mean H_{m0} obtained with the RHTestsV4 methodology. All change points are found before 2002, which coincides with the periods in which there were more failures in observations. These gaps in data acquisition that occurred in the previous two decades could be responsible for the changepoints detected, particularly Type 1 points for which there is no historical evidence of buoy switch or any updated at the processing level.

Applying a homogenization technique requires knowing very well all the changes in the measurement procedures and data analysis that occurred since the wave buoys started to operate. For about 40 years of wave records, this typically includes changes in buoys, processing software and parameters. This is a usual process due to technological advances and buoys deterioration. The reality is that it is practically impossible to have long-term measurements (at decadal scales) without changes that could affect the interpretation of long-term analysis. Another challenge is related to intergenerational changes as buoy operators retire and useful metadata can be lost if not properly reported.

4.2. Wave trends offshore mainland portugal

The wind-wave trend analyses presented in this study showed important differences even at relatively small spatial distances (< 500 km). As an example, while wind-wave trends from FigLei and Faro records displayed statistically significant values, the Sines record did not display such statistically significant trends. It is well known that FigLei and Faro records were obtained in different wave climate conditions. While FigLei record is often subjected to north-western and western wave storms generated in the North Atlantic Ocean (IM, 2004), the Faro record is also subjected to sea states generated in the Mediterranean Sea (Oliveira et al., 2018). In regards the differences between FigLei and Sines records, they were obtained from buoys that are moored along the western coastline, thereby subjected to similar wind-wave conditions. Nevertheless, Sines record shows a milder wave climate and with mean wave directions slightly rotated towards west (e.g., Dodet et al., 2010; Oliveira et al., 2018). Moreover, the maximum values of H_{m0} during post-tropical storms that cross mainland Portugal can be markedly different between FigLei and Sines records (Oliveira et al., 2020). The above-mentioned differences between FigLei and Sines records can provide support to the obtained differences of wind-wave trends obtained in this study.

Our analysis showed differences and similarities when compared to previous studies. Unlike Bacon & Carter (1991) and Bertin et al. (2013), we did not find any statistically significant trend in the annual monthly mean H_{m0} offshore mainland Portugal. This difference might be due not only to the distinct latitudes between mainland Portugal and the Seven Stones Light Vessel but also due to different time periods of each dataset. Our analysis of January H_{m0} at Faro yielded contrasting results compared with the increase of +120.0 mm/yr by Sterl et al. (1998).

We observed statistically significant decreasing trend for both monthly mean H_{m0} (−10.7 mm/yr) and for the monthly 90-percentile of H_{m0} (−21.2 mm/yr) (see Appendix B). Nevertheless, our results further substantiate the trends spatial variability in the North Atlantic as already pointed out by previous authors. Looking at the results of Wang and Swail (2001), our study does not show any statistically significant trends during JFM. The only trend in our study is the +2.8 mm/yr increase in monthly 10-percentile of H_{m0} at Faro. Similar to Dodet et al. (2010), we did find a decreasing trend of −16.5 mm/yr at Faro for the semi-annual winter period (October to March).

For the winter months (DJFM), increasing trends were observed at FigLei but only statistically significant at 90 % level. In more details, both the monthly mean H_{m0} and the monthly 90-percentile increased by +10.3 mm/yr and +15.3 mm/yr, respectively. An increase was also observed for Faro but for the monthly 10-percentile (+3.1 mm/yr). These results are in agreement with those presented by Martínez-Asensio et al. (2016). Note that part of the above-mentioned differences may also arise from the different time periods associated with each study.

When comparing our results with satellite altimetry studies performed by Young and Ribal (2019) and Hochet et al. (2021), our results agree with their results for this region of the North Atlantic Ocean with no statically significant trends in the annual records.

Our results show agreements and differences with previous regional and global studies performed with several methods, such as instrumental measurements, numerical model wave hindcasts and satellite altimetry. An important aspect of wave trends in the North Atlantic is their spatial variability between higher and lower latitudes, as previously noticed by Günther et al. (1997), Sterl et al. (1998) and Wang & Swail (2001). Our results further point out that these differences can be vary localized in space. As an example, while the monthly 90-percentile H_{m0} is decreasing (−22.2 mm/yr) for the OND quarter on Faro record, located in the southern coastline, this parameter is increasing (+15.3 mm/yr) for the DJFM period in FigLei record, located in the north-western coastline.

When compared wave buoy records and ERA5 wave hindcast, our results suggest the following. While the decreasing or increasing trend is well captured by ERA5 wave hindcast, the rate or the statistical significance is not. Two examples include the monthly 90-percentile for Faro record during the OND quarter and the 90-percentile for FigLei record in the DJFM period. At Faro, the wave buoy data shows a decreasing trend of −22.2 mm/yr while the ERA5 hindcast shows a −2.2 mm/yr (Fig. 6d).

The FigLei record displays an increasing trend of +15.2 mm/yr while the ERA5 wave hindcast displays a + 2.5 mm/yr (Fig. 6e). This comparison points out that even if the ERA5 wave hindcast trends offshore mainland Portugal may not be statistically significant, they can underestimate by up to a factor of 10 the observed wave trends. Nevertheless, our results suggest that ERA5 wave hindcast correctly reproduces the upward or downward observed wave trends. In future, these differences may be reduced if machine learning algorithms (Lucero et al., 2023) or calibration methods (Fanti et al., 2023) are used to improve global wave hindcasts. Nevertheless, both methodologies require long-term wave buoy networks.

Our analysis is hereafter compared with other studies that used climate data based on a particular gas-emission scenario to compute the wave trends until the end of the 21st century. A particular example is the study performed by Bernardino et al. (2023). In that study, the authors used a numerical phase-averaged model forced by winds with a spatial resolution of 0.5° (i.e. about 55 km at the Equator) and a time resolution of 3 h. The wind fields were provided with an earth-system model, called EC-Earth. The results obtained in Bernardino et al. (2023) for the present climate can be compared with those obtained in the present study. In more details, the general decrease (or no change) of mean H_{m0} is observed in our dataset at the south-western coastline as well as the west coast, where no statistically significant annual trends were observed.

4.3. Practical implications of the results

Our results can have practical implications to the design of maritime structures. For instance, regarding breakwater design, our trends only support an increase of design wave height due to increasing trends of monthly 90-percentile H_{m0} values at 90 % level (Fig. 6c-e). Interestingly, the design wave height may even decrease, when considering the months between October and December at Faro (−22.2 mm/yr). Therefore, we propose that along mainland Portugal if the breakwater is located under depth-limited conditions for the design wave height, the projected increase in the sea level rise may have a more important effect for the design wave height than the offshore increase of the design wave height itself. A key novelty of this study is the analysis of the monthly 10-percentile H_{m0}, which has not been widely explored in previous research. This parameter has an increasing trend for OND for FigLei record (+6.7 mm/yr) and for the annual period at Faro (+2.5 mm/yr). Although the precise impact of the monthly 10-percentile H_{m0} is not clearly understood, it may indicate some effect on the coastal morphodynamics and on harbour or marina logistics. The implications of the obtained trends in monthly 10-percentile H_{m0} for human related activities may constitute a topic of future research.

5. conclusions

Long-term trends in monthly mean, 90-percentile and 10-percentile H_{m0} were analysed based on wave buoy records obtained offshore mainland Portugal. For such purpose, a homogenized technique was applied to these records to remove non-climatic step changes. From this study, the following conclusions can be drawn:

1. Non-climatic step changes associated with the long-term wave buoy network (spanning 40 years) located at about 100 m water depth are smaller than 0.16 m.A possible reason for this very small value can be associated with the manufacturer of the wave buoys, which was the same throughout the years. Nevertheless, maintaining a singular, consistent buoy system and rigorously adhering to identical data processing algorithms over decades presents significant logistical and technical challenges. Consequently, significant wave height datasets exhibiting small step changes over such a long duration are difficult to find, making the data from the IH wave buoy network offshore mainland Portugal particularly valuable for long-term wave analysis and research. Furthermore, the quality and consistency of the dataset analysed in this study make it highly suitable for the calibration and validation of wave hindcast models and wave climate models;
2. Statistically significant trends at 95 % level were observed at the northwestern coast (FigLei), at the southern coast (Faro) but not at the southwestern coast (Sines). On the FigLei record, the monthly mean H_{m0} increased by +10 mm/yr for the months between October and December. At Faro, the annual monthly 10-percentile H_{m0} increased by +2.5 mm/yr and the winter monthly 90-percentile H_{m0} decreased by −16.5 mm/yr. Interestingly, the monthly 90-percentile H_{m0} increased by +15.2 mm/yr on the FigLei record for the months between December and March but this value is statistically significant at 90 % level;
3. The comparison between our results with those obtained in previous studies for the North Atlantic and with ERA5 wave hindcast showed differences and similarities. Our results indicate that ERA5 wave hindcast can provide the correct increasing or decreasing wave trends. However, the rates can be underestimated by up to a factor of 10 and they were not statistically significant, in general.

By documenting the changes in one of the world's longest continuous wave buoy observation networks, this research provides valuable insights for current and future ocean researchers and engineers. It also emphasizes the urgent need for standardized reporting practices to ensure the integrity and comparability of long-term wave buoy measurements. Such standardized practices will enhance the reliability and comparability of wave data across different time periods and locations, ultimately advancing our understanding of long-term wave climate variability and its implications for ocean management and engineering.

Data availability

The data that support the findings of this study are available in the following ZENODO repository (https://zenodo.org/records/12782516; DOI: 10.5281/zenodo.12782516). ERA5 wave hindcast is publicly available through the Copernicus Climate Data Store (https://cds.climate.copernicus.eu/#!/home).

CRediT authorship contribution statement

Rita Esteves: Writing – original draft, Methodology, Investigation, Formal analysis, Conceptualization. **Diogo Mendes:** Writing – original draft, Methodology, Investigation, Formal analysis. **Maria Graça Neves:** Writing – review & editing, Methodology. **Tiago Oliveira:** Writing – review & editing, Methodology. **José Paulo Pinto:** Writing – review & editing, Methodology, Investigation, Formal analysis, Conceptualization.

Declaration of competing interest

The authors declare that they have no known competing financial interests or personal relationships that could have appeared to influence the work reported in this paper.

Acknowledgements

We gratefully acknowledge Instituto Hidrográfico for their support to the MONIZEE network. We would also like to express our appreciation to Administração do Porto de Sines e do Algarve (APS S.A.) and Administração do Porto do Douro e Leixões (APDL) for their commitment to maintaining the buoys located in Sines, Faro, and Leixões. DM and MGN are grateful for the Foundation for Science and Technology's support through funding UIDB/04625/2020 from the research unit CERIS (DOI: 10.54499/UIDB/04625/2020). The authors acknowledge Jeff Burkey for making publicly available the computer routine to compute the Mann-Kendall test and the Sen's slope (http://www.mathworks.com/matlabcentral/fileexchange/authors/23983). The authors thank three anonymous reviewers for providing us with valuable comments that have resulted in an improved paper.

Appendix A

The error metrics used in this paper, introduced by Willmott et al. (1985), include the average difference between simulations (i.e., ERA5 hindcast) and observations (i.e., buoy data) – BIAS; the root mean square error – RMSE; and the root mean square error normalized by the mean value of the observations – NRMSE, as follows:

$$BIAS = \frac{1}{N}\sum_{i=1}^{N}(sim_i - obs_i)$$

$$RMSE = \sqrt{\frac{1}{N}\sum_{i=1}^{N}(sim_i - obs_i)^2}$$

$$NRMSE = \frac{RMSE}{\frac{1}{N}\sum_{i=1}^{N} obs_i}$$

Appendix B

Table B1, Table B2, Table B3, Table B4

Table B1
– Annual wind-wave trends of monthly H_{m0} for wave buoy records and ERA5 hindcast.

		Wave buoy records			*ERA5 wave hindcast*		
		90-percentile	*mean*	*10-percentile*	*90-percentile*	*mean*	*10-percentile*
FigLei	*mm/yr*	+1.5	+0.8	+1.8	+4.1	+2.3	+1.3
	p-value	0.7000	0.45000	0.7300	0.1100	0.0874	0.2134
Sines	*mm/yr*	−3.9	−0.4	+0.1	+3.0	+2.7	+2.5
	p-value	0.4200	0.8700	0.8700	0.4012	0.0363	0.0211
Faro	*mm/yr*	−1.0	+1.4	+2.5	+0.3	+0.7	+0.9
	p-value	0.8300	0.4400	0.0070	0.9355	0.2060	0.0108

Table B2
– Semi-annual wind-wave trends of monthly H_{m0} for wave buoy records and ERA5 hindcast.

ONDJFM		*Wave buoy records*			*ERA5 wave hindcast*		
		90-percentile	*mean*	*10-percentile*	*90-percentile*	*mean*	*10-percentile*
FigLei	*mm/yr*	+9.3	+6.0	+3.6	+3.4	+3.1	+2.0
	p-value	0.4415	0.2480	0.2342	0.3151	0.2287	0.2245
Sines	*mm/yr*	−4.2	−1.7	+1.5	+1.7	+2.6	+2.1
	p-value	0.3812	0.7398	0.6946	0.6008	0.2810	0.2495
Faro	*mm/yr*	−16.5	−3.3	+1.6	−1.9	+0.2	+0.8
	p-value	0.0252	0.2174	0.1439	0.2583	0.8342	0.1736
AMJJAS		*Wave buoy records*			*ERA5 wave hindcast*		
		90-percentile	*mean*	*10-percentile*	*90-percentile*	*mean*	*10-percentile*
FigLei	*mm/yr*	+1.3	+1.6	+0.9	+0.3	+1.1	+2.1
	p-value	0.7212	0.4957	0.7951	0.8954	0.3679	0.0391
Sines	*mm/yr*	+1.0	+1.3	+0.9	+2.1	+2.3	+2.5
	p-value	0.7914	0.3211	0.5968	0.1480	0.0228	0.0067
Faro	*mm/yr*	+0.5	+1.2	+1.8	+1.7	+1.1	+0.6
	p-value	0.9407	0.4419	0.0150	0.0363	0.0462	0.0409

Table B3
– Quarter wind-wave trends of monthly H_{m0} for wave buoy records and ERA5 hindcast.

JFM		*Wave buoy records*			*ERA5 wave hindcast*		
		90-percentile	*mean*	*10-percentile*	*90-percentile*	*mean*	*10-percentile*
FigLei	*mm/yr*	+6.7	+0.8	−2.4	+5.2	+2.3	+0.4
	p-value	0.2336	0.8700	0.6572	0.4361	0.5919	0.9355
Sines	*mm/yr*	−5.3	+2.2	+2.3	+4.2	+2.7	−0.3
	p-value	0.5878	0.6920	0.3926	0.4915	0.4602	0.8634
Faro	*mm/yr*	−7.6	−2.0	+2.8	−0.7	+1.0	+0.4

(continued on next page)

Table B3 (*continued*)

JFM		*Wave buoy records*			*ERA5 wave hindcast*		
		90-percentile	*mean*	*10-percentile*	*90-percentile*	*mean*	*10-percentile*
	p-value	0.3042	0.4646	0.0283	0.8318	0.4979	0.6128
AMJ		*Wave buoy records*			*ERA5 wave hindcast*		
		90-percentile	*mean*	*10-percentile*	*90-percentile*	*mean*	*10-percentile*
FigLei	*mm/yr*	−2.7	−3.9	−1.8	−0.6	+0.8	+1.5
	p-value	0.4834	0.2825	0.4270	0.8954	0.5506	0.2325
Sines	*mm/yr*	+2.3	+2.7	+1.8	+2.9	+2.2	+2.7
	p-value	0.4460	0.0692	0.2297	0.4184	0.0950	0.0156
Faro	*mm/yr*	+3.0	+1.9	+2.2	+2.4	+1.7	+0.8
	p-value	0.5236	0.1107	0.0015	0.0717	0.0189	0.0216
JAS		*Wave buoy records*			*ERA5 wave hindcast*		
		90-percentile	*mean*	*10-percentile*	*90-percentile*	*mean*	*10-percentile*
FigLei	*mm/yr*	+0.0	+1.7	+2.1	−0.7	+1.0	+2.2
	p-value	0.9842	0.4893	0.2356	0.7309	0.5506	0.1122
Sines	*mm/yr*	−1.4	−0.2	+0.5	+0.9	+1.7	+2.3
	p-value	0.7466	0.8783	0.7725	0.6709	0.1657	0.0328
Faro	*mm/yr*	−2.2	−0.3	+1.3	+0.7	+0.5	+0.4
	p-value	0.5180	0.8674	0.0603	0.2564	0.2738	0.2206
OND		*Wave buoy records*			*ERA5 wave hindcast*		
		90-percentile	*mean*	*10-percentile*	*90-percentile*	*mean*	*10-percentile*
FigLei	*mm/yr*	+10.0	+10.0	+6.7	+3.8	+5.0	+2.8
	p-value	0.2266	0.0476	0.0799	0.3850	0.1318	0.1872
Sines	*mm/yr*	+3.3	+5.4	+3.2	+2.6	+3.8	+2.7
	p-value	0.8948	0.4806	0.3899	0.6302	0.2207	0.1486
Faro	*mm/yr*	−22.2	−7.1	+3.3	−2.2	+0.4	+1.1
	p-value	0.0484	0.2713	0.0753	0.4024	0.8260	0.2245

Table B4
- Quarterly wind-wave trends of monthly H_{m0} for wave buoy records and ERA5 hindcast.

DJFM		*Wave buoy records*			*ERA5 wave hindcast*		
		90-percentile	*mean*	*10-percentile*	*90-percentile*	*mean*	*10-percentile*
FigLei	*mm/yr*	+15.3	+10.3	+2.8	+2.5	+2.1	+1.3
	p-value	0.0813	0.0538	0.2908	0.6755	0.5719	0.5791
Sines	*mm/yr*	−3.3	+0.0	+1.9	−1.0	+1.6	+1.3
	p-value	0.4874	0.9759	0.6946	0.8670	0.6081	0.4895
Faro	*mm/yr*	−6.7	−0.5	+3.1	−3.0	+0.2	+0.8
	p-value	0.2906	0.9278	0.0217	0.3681	0.9333	0.2669

References

Aarnes, O.J., Reistad, M., Breivik, Ø., Bitner-Gregersen, E., Ingolf Eide, L., Gramstad, O., et al., 2017. Projected changes in significant wave height toward the end of the 21st century: northeast A tlantic. Journal of Geophysical Research: Oceans 122 (4), 3394–3403. https://doi.org/10.1002/2016JC012521.

Bacon, S., Carter, D.J.T., 1991. Wave climate changes in the North Atlantic and North Sea. International Journal of Climatology 11 (5), 545–558. https://doi.org/10.1002/joc.3370110507.

Bernardino, M., Gonçalves, M., Campos, R.M., Guedes Soares, C., 2023. Extremes and variability of wind and waves across the oceans until the end of the 21st century. Ocean Engineering 275, 114081. https://doi.org/10.1016/j.oceaneng.2023.114081.

Bertin, X., Prouteau, E., Letetrel, C., 2013. A significant increase in wave height in the North Atlantic Ocean over the 20th century. Glob. Planet. Change 106, 77–83. https://doi.org/10.1016/j.gloplacha.2013.03.009.

Bitner-Gregersen, E.M., Vanem, E., Gramstad, O., Hørte, T., Aarnes, O.J., Reistad, M., et al., 2018. Climate change and safe design of ship structures. Ocean Engineering 149, 226–237. https://doi.org/10.1016/j.oceaneng.2017.12.023.

Bricheno, L.M., Wolf, J., 2018. Future Wave Conditions of Europe, in Response to High-End Climate Change Scenarios. Journal of Geophysical Research: Oceans 123 (12), 8762–8791. https://doi.org/10.1029/2018JC013866.

Campos, R.M., Bernardino, M., Gonçalves, M., Guedes Soares, C., 2022. Assessment of metocean forecasts for Hurricane Lorenzo in the Azores Archipelago. Ocean Engineering 243, 110292. https://doi.org/10.1016/j.oceaneng.2021.110292.

Casas-Prat, M., Hemer, M.A., Dodet, G., Morim, J., Wang, X.L., Mori, N., et al., 2024. Wind-wave climate changes and their impacts. Nature Reviews Earth & Environment 5 (1), 23–42. https://doi.org/10.1038/s43017-023-00502-0.

Cavaleri, L., Abdalla, S., Benetazzo, A., Bertotti, L., Bidlot, J.-R., Breivik, Ø., et al., 2018. Wave modelling in coastal and inner seas. Prog. Oceanogr. 167, 164–233. https://doi.org/10.1016/j.pocean.2018.03.010.

CIRIA/CUR/CETMEF, 2007. The Rock Manual. The use of rock in hydraulic engineering C683.

Clemente, D., Rosa-Santos, P., Ferradosa, T., Taveira-Pinto, F., 2023. Wave energy conversion energizing offshore aquaculture: prospects along the Portuguese coastline. Renew. Energy 204, 347–358. https://doi.org/10.1016/j.renene.2023.01.009.

DNV-RP-C205, 2019. Environmental conditions and environmental loads.

Dodet, G., Bertin, X., Taborda, R., 2010. Wave climate variability in the North-East Atlantic Ocean over the last six decades. Ocean. Model. (Oxf) 31 (3–4), 120–131. https://doi.org/10.1016/j.ocemod.2009.10.010.

Fanti, V., Ferreira, Ó., Kümmerer, V., Loureiro, C., 2023. Improved estimates of extreme wave conditions in coastal areas from calibrated global reanalyses. Commun. Earth. Environ. 4 (1), 151. https://doi.org/10.1038/s43247-023-00819-0.

Gemmrich, J., Thomas, B., Bouchard, R., 2011. Observational changes and trends in northeast Pacific wave records: NE PACIFIC WAVE TRENDS. Geophys. Res. Lett. 38 (22). https://doi.org/10.1029/2011GL049518 n/a-n/a.

Günther, H., Rosenthal, W., Stawarz, M., Carretero, J., Gomez, M., Lozano, I., et al., 1997. The wave climate of the Northeast Atlantic over the period 1955-1994: the WASA wave hindcast. GKSS-Forschungszentrum Geesthacht GmbH.

Hersbach, H., Bell, B., Berrisford, P., Hirahara, S., Horányi, A., Muñoz-Sabater, J., et al., 2020. The ERA5 global reanalysis. Quart. J. Royal Meteorological Soc. 146 (730), 1999–2049. https://doi.org/10.1002/qj.3803.

Hochet, A., Dodet, G., Ardhuin, F., Hemer, M., Young, I., 2021. Sea State Decadal Variability in the North Atlantic: a Review. Climate 9 (12), 173. https://doi.org/10.3390/cli9120173.

IM. (2004). Caracterização Climática da Costa - Características do Clima da Costa de Portugal Continental. Technical Report (in Portuguese).
Kodaira, T., Sasmal, K., Miratsu, R., Fukui, T., Zhu, T., Waseda, T., 2023. Uncertainty in wave hindcasts in the North Atlantic Ocean. Marine Structures 89, 103370. https://doi.org/10.1016/j.marstruc.2023.103370.
Law-Chune, S., Aouf, L., Dalphinet, A., Levier, B., Drillet, Y., Drevillon, M., 2021. WAVERYS: a CMEMS global wave reanalysis during the altimetry period. Ocean. Dyn. 71 (3), 357–378. https://doi.org/10.1007/s10236-020-01433-w.
Liu, J., Meucci, A., Young, I.R., 2023. A Comparison of Multiple Approaches to Study the Modulation of Ocean Waves Due To Climate Variability. Journal of Geophysical Research: Oceans 128 (9), e2023JC019843. https://doi.org/10.1029/2023JC019843.
Lucero, F., Stringari, C.E., Filipot, J.-F., 2023. Improving WAVEWATCH III hindcasts with machine learning. Coast. Eng. 185, 104381. https://doi.org/10.1016/j.coastaleng.2023.104381.
Mann, H.B., 1945. Nonparametric Tests Against Trend. Econometrica 13 (3), 245. https://doi.org/10.2307/1907187.
Martínez-Asensio, A., Marcos, M., Tsimplis, M.N., Jordà, G., Feng, X., Gomis, D., 2016. On the ability of statistical wind-wave models to capture the variability and long-term trends of the North Atlantic winter wave climate. Ocean. Model. (Oxf) 103, 177–189. https://doi.org/10.1016/j.ocemod.2016.02.006.
Masselink, G., Castelle, B., Scott, T., Dodet, G., Suanez, S., Jackson, D., Floc'h, F., 2016. Extreme wave activity during 2013/2014 winter and morphological impacts along the Atlantic coast of Europe. Geophys. Res. Lett. 43 (5), 2135–2143. https://doi.org/10.1002/2015GL067492.
Mendes, D., Oliveira, T.C.A., 2021. Deep-water spectral wave steepness offshore mainland Portugal. Ocean Engineering 236, 109548. https://doi.org/10.1016/j.oceaneng.2021.109548.
Meucci, A., Young, I.R., Hemer, M., Trenham, C., Watterson, I.G., 2023. 140 Years of Global Ocean Wind-Wave Climate Derived from CMIP6 ACCESS-CM2 and EC-Earth3 GCMs: global Trends, Regional Changes, and Future Projections. J Clim 36 (6), 1605–1631. https://doi.org/10.1175/JCLI-D-21-0929.1.
Morim, J., Trenham, C., Hemer, M., Wang, X.L., Mori, N., Casas-Prat, M., et al., 2020. A global ensemble of ocean wave climate projections from CMIP5-driven models. Sci. Data 7 (1), 105. https://doi.org/10.1038/s41597-020-0446-2.
Oliveira, T.C.A., Neves, M.G., Fidalgo, R., Esteves, R., 2018. Variability of wave parameters and H/H relationship under storm conditions offshore the Portuguese continental coast. Ocean Engineering 153, 10–22. https://doi.org/10.1016/j.oceaneng.2018.01.080.
Oliveira, T.C.A., Cagnin, E., A. Silva, P., 2020. Wind-waves in the coast of mainland Portugal induced by post-tropical storms. Ocean Engineering 217, 108020. https://doi.org/10.1016/j.oceaneng.2020.108020.
Ponce De León, S., Guedes Soares, C., 2014. Extreme wave parameters under North Atlantic extratropical cyclones. Ocean. Model. (Oxf) 81, 78–88. https://doi.org/10.1016/j.ocemod.2014.07.005.
Ponce De León, Sonia, Guedes Soares, C., 2015. Hindcast of the Hércules winter storm in the North Atlantic. Natural Hazards 78 (3), 1883–1897. https://doi.org/10.1007/s11069-015-1806-7.
Ribeiro, A.S., deCastro, M., Rusu, L., Bernardino, M., Dias, J.M., Gomez-Gesteira, M., 2020. Evaluating the Future Efficiency of Wave Energy Converters along the NW Coast of the Iberian Peninsula. Energies. (Basel) 13 (14), 3563. https://doi.org/10.3390/en13143563.
Ruggiero, P., Komar, P.D., Allan, J.C., 2010. Increasing wave heights and extreme value projections: the wave climate of the U.S. Pacific Northwest. Coast. Eng. 57 (5), 539–552. https://doi.org/10.1016/j.coastaleng.2009.12.005.
Sen, P.K., 1968. Estimates of the Regression Coefficient Based on Kendall's Tau. J. Am. Stat. Assoc. 63 (324), 1379–1389. https://doi.org/10.1080/01621459.1968.10480934.
Silva, K., Abreu, T., Oliveira, T.C.A., 2022. Inter- and intra-annual variability of wave energy in Northern mainland Portugal: application to the HiWave-5 project. Energy Reports 8, 6411–6422. https://doi.org/10.1016/j.egyr.2022.05.005.
Sterl, A., Komen, G.J., Cotton, P.D., 1998. Fifteen years of global wave hindcasts using winds from the European Centre for Medium-Range Weather Forecasts reanalysis: validating the reanalyzed winds and assessing the wave climate. Journal of Geophysical Research: Oceans 103 (C3), 5477–5492. https://doi.org/10.1029/97JC03431.
Stopa, J.E., Ardhuin, F., Stutzmann, E., Lecocq, T., 2019. Sea State Trends and Variability: consistency Between Models, Altimeters, Buoys, and Seismic Data (1979–2016). Journal of Geophysical Research: Oceans 124 (6), 3923–3940. https://doi.org/10.1029/2018JC014607.
Taskar, B., Sasmal, K., Yiew, L.J., 2023. A case study for the assessment of fuel savings using speed optimization. Ocean Engineering 274, 113990. https://doi.org/10.1016/j.oceaneng.2023.113990.
UNESCO, 1993. Manual of Quality Control Procedures For Validation of Oceanographic Data. Manual and Guides.
U.S. Integrated Ocean Observing System. (2019). Manual for Real-Time Quality Control of In-Situ Surface Wave Data: a Guide to Quality Control and Quality Assurance of In-Situ Surface Wave Observations Version 2.1. https://doi.org/10.25923/7YC5-VS69.
Vincent, L.A., Wang, X.L., Milewska, E.J., Wan, H., Yang, F., Swail, V., 2012. A second generation of homogenized Canadian monthly surface air temperature for climate trend analysis. Journal of Geophysical Research: Atmospheres (D18), 117. https://doi.org/10.1029/2012JD017859, 2012JD017859.
Wang, X., Feng, Y., 2013. RHTestsV4 User Manual. Climate Research Division, Atmospheric Science and Technology Directorate, Science and Technology Branch, Environment Canada.
Wang, X.L., 2008. Accounting for Autocorrelation in Detecting Mean Shifts in Climate Data Series Using the Penalized Maximal t or F Test. J. Appl. Meteorol. Climatol. 47 (9), 2423–2444. https://doi.org/10.1175/2008JAMC1741.1.
Wang, X.L., Swail, V.R., 2001. Changes of Extreme Wave Heights in Northern Hemisphere Oceans and Related Atmospheric Circulation Regimes. J Clim 14 (10), 2204–2221. https://doi.org/10.1175/1520-0442(2001)014<2204:COEWHI>2.0.CO;2.
Wang, X.L., Wen, Q.H., Wu, Y., 2007. Penalized Maximal t Test for Detecting Undocumented Mean Change in Climate Data Series. J. Appl. Meteorol. Climatol. 46 (6), 916–931. https://doi.org/10.1175/JAM2504.1.
Wang, X.L., Chen, H., Wu, Y., Feng, Y., Pu, Q., 2010. New Techniques for the Detection and Adjustment of Shifts in Daily Precipitation Data Series. J. Appl. Meteorol. Climatol. 49 (12), 2416–2436. https://doi.org/10.1175/2010JAMC2376.1.
Willmott, C.J., Ackelson, S.G., Davis, R.E., Feddema, J.J., Klink, K.M., Legates, D.R., O'Donnell, J., Rowe, C.N., 1985. Statistics for the evaluation and comparison of model. J. Geophys. Res. 90 (C5), 8995–9005. https://doi.org/10.1029/JC090iC05p08995.
Young, I.R., Ribal, A., 2019. Multiplatform evaluation of global trends in wind speed and wave height. Science (1979) 364 (6440), 548–552. https://doi.org/10.1126/science.aav9527.